

The road to energy-efficient optical access: GreenTouch final results

Sofie Lambert, Prasanth Ananth, Peter Vetter, Ka-Lun Lee, Jie Li, Xin Yin, Hungkei Chow, Jean-Patrick Gelas, Laurent Lefèvre, Dominique Chiaroni, Bart Lannoo, and Mario Pickavet

Abstract—The growing energy footprint of communication networks has raised concern about the sustainability of future network development. The GreenTouch consortium was founded to help counter this trend by developing and integrating green network technologies from the access to the core. In order to evaluate these technologies, an end-to-end network power model was developed in the form of the Green Meter, a tool to assess the overall impact and overall energy efficiency benefits from an entire portfolio of solutions. In this paper, we describe the methodology of the Green Meter for the residential fixed access portion, which was extended to include metro aggregation. A baseline architecture for optical access and metro aggregation networks is defined, and adapted to other scenarios integrating future technologies. The performance is each time evaluated through a mathematical model that captures the energy savings at the component level and has the ability to compute the overall system-level energy savings. We show that energy efficiency can be improved 29-fold over a decade (2010-2020) with business-as-usual trends, and with the added effort of introducing GreenTouch solutions, this could be further improved to achieve a 257-fold increase in energy efficiency. The results confirm that an emphasis on green network design can indeed have a huge impact on reducing the energy consumption of optical access infrastructure.

Index Terms—energy efficiency, next-generation passive optical network, GreenTouch.

I. INTRODUCTION AND MOTIVATION

COMMUNICATION networks have grown tremendously over the past decades, becoming more widespread, offering higher rates, and better performance. This has however come at a large energy cost. Worldwide electricity consumption by communication networks grew at an annual rate of 10% from 2007 to 2012 [1]. When this problem became apparent, several large international research projects were initiated to foster a more sustainable growth of communication networks: examples include TREND, EARTH, ECONET, STRONGEST, and GreenTouch.

S. Lambert, X. Yin, B. Lannoo, and M. Pickavet are with the Department of Information Technology, Ghent University - iMinds/IMEC, Ghent, Belgium. e-mail: firstname.lastname@intec.ugent.be

P. Ananth, P. Vetter, and H. Chow are with Nokia Bell Labs, Fixed Networks, Murray Hill, NJ, US.

K. L. Lee and J. Li are with the Centre for Energy-efficient Telecommunications (CEET), University of Melbourne, VIC, Australia.

J.-P. Gelas is with Université Claude Bernard Lyon 1 - INRIA - École Normale Supérieure de Lyon, France

L. Lefèvre is with INRIA - École Normale Supérieure de Lyon, France.

D. Chiaroni is with Nokia Bell Labs, IP and Optical Networks, Centre de Villarceaux, Nozay, France.

Manuscript received June 4, 2016; revised Month DD, YYYY.

The GreenTouch consortium was founded in 2010 with the ambitious goal to improve the energy efficiency of communication networks by a factor 1000x by 2020. At the conclusion of the project in 2015, the outcome of a comprehensive research study, called the *Green Meter*, was published [2]. The Green Meter assesses the overall impact and overall energy efficiency benefits from an entire portfolio of solutions investigated and developed by GreenTouch. The results are not limited to the energy benefits of a single technology, but instead focus on an end-to-end network perspective including a full range of technologies, and accounting for future traffic growth. It was shown that a 98% reduction of the net energy consumption in end-to-end communications networks can be achieved by 2020 compared to the 2010 reference scenario.

In this paper, we describe the methodology that was used to obtain the residential fixed access portion of the Green Meter results in detail. We quantify the effect of different energy-saving approaches on the main sub-systems such as the optical network unit (ONU) and the optical line terminal (OLT), each time expressing it in a corresponding saving factor. We also include the metro aggregation network containing the aggregation switch (AS) and the edge router (ER) in our model, allowing us to evaluate the effect of technologies bypassing the local exchange, thus extending the reach of the access network. In the rest of this work, when we refer to the access, we always mean the extended version, including the metro aggregation.

The proposed methodology is applied to three scenarios:

- 1) Baseline 2010: using the most energy-efficient commercially deployed technologies at the start of GreenTouch in 2010;
- 2) business-as-usual (BAU) 2020: using similar technologies as in the baseline scenario, assuming energy efficiency is improved following current technological trends until 2020;
- 3) GreenTouch (GT) 2020: leveraging novel GreenTouch architecture and technologies together with non-BAU techniques that are expected to be available by 2020.

Preliminary results of the Green Meter for fixed access have previously been published in two conference papers [3], [4]. The main updates in the present work are the direct inclusion of cascaded bit-interleaving (CBI) and point-to-point (PtP) in the GT architecture; the extension of the model to include metro aggregation; updates to the saving factors based on demonstrated savings for CBI, PtP, and virtual home gateway (vHGW); updated sleep saving estimates; accounting for man-

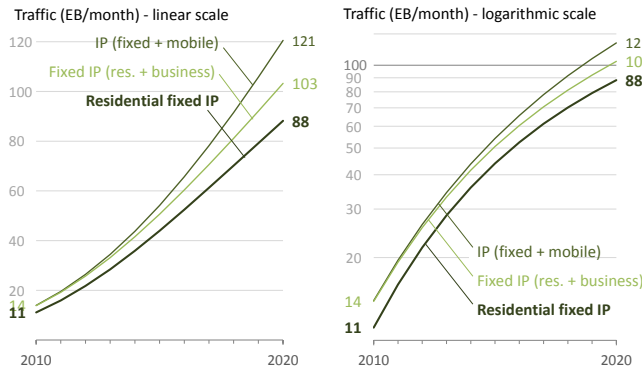


Fig. 1. Projected traffic (in exabytes/month) for Group 1 countries (North America, Western Europe and Japan), shown on a linear and logarithmic scale. A hyperbolically decreasing CAGR was fitted to historical traffic trends to obtain the projections [5].

aged Internet Protocol (IP) traffic in network dimensioning; revised cooling overheads; and further improvements in the way we account for supply transition, Moore’s law, and power shedding.

The paper is organized as follows. We start with an overview of the expected traffic growth in fixed access in Section II. Next we introduce the baseline, BAU (Section II) and GT architectures (Section III), and briefly describe the concepts behind a number of disruptive technologies that are used in the GT scenario (Section III). A detailed description of the Green Meter model follows in Section IV, introducing the saving factors for all energy-saving approaches and how they can be combined. Finally, we apply the model to obtain results for the three scenarios mentioned above in Section V. Conclusions are drawn in Section VI.

II. EXPECTED EVOLUTION OF COMMUNICATION NETWORKS

A. Traffic trends

Traffic growth and growing numbers of subscribers are the two main drivers of growing power consumption in communication networks. In order to properly dimension a future-proof network and assess its energy efficiency, we first need to determine how much traffic will be passing through it.

The GreenTouch Services, Policies and Standards (SPS) group developed traffic volume and growth projections from 2010 to 2020 based on regression analysis of historical trends. The projections build on a semi-empirical model in which traffic growth does not follow an exponential trend with a fixed compound annual growth rate (CAGR), but instead exhibits a CAGR that hyperbolically decreases over time [5]. Fitting this model to historical trends and near-term forecasts that were available at the time of the SPS analysis [6], [7] results in the GreenTouch projections shown in Figure 1.

The traffic projections and network models are developed for the mature markets of North America, Western Europe and Japan (also called *Group 1 countries*) rather than for worldwide markets, because more reliable data is available for Group 1 countries, and to avoid methodological issues from population growth and having to account for limited electricity

grid availability in our network design. In this work, when we refer to total traffic volumes and subscriber numbers, we are always considering Group 1 countries.

The three lines in Figure 1 show the GreenTouch estimates for overall IP traffic (top), the fixed access contribution (middle), and finally the residential portion of fixed access (bottom)¹. Although the mobile share in overall IP traffic is on the rise, illustrated by the growing distance between the top and middle curve, fixed access will continue to be the main source of IP traffic until 2020 and beyond, and the total traffic volume passing the fixed access network will grow by a factor 7.5x between 2010 and 2020. Since this work deals with residential access networks, the most relevant trend for our further analysis is that of residential fixed access traffic, which will grow almost 8-fold from an estimated 11 EB/month in 2010 to 88 EB/month in 2020 (1 EB = 1 exabyte = 1 billion gigabytes).

Independent of the traffic analyses, the number of residential fixed subscribers was projected to 2020 by the SPS group based on similar regression analyses for years prior to 2012 [8]. Values for 2010 and 2020 are shown in Table I.

B. Implications for network design

The dimensioning of the access network depends on the provisioned data rate per subscriber. The traffic and subscriber projections from the previous section are combined to calculate the average total bit rate per subscriber in Table I.

Further, we need to know the downstream (DS) and upstream (US) component of this average bit rate. This requires the DS/US ratio of residential traffic in 2010 and 2020, which is obtained by calculating a weighted average of appropriate DS/US weights for various traffic sub-components based on the type of service². The resulting ratio increases from 79/21 to 83/17 over the years, mainly due to the growing importance of downstream-heavy video traffic. So throughout the period under study, downstream traffic imposes higher bandwidth requirements on the network than upstream. This is not only the case in the network uplinks, which are symmetric, but also in the passive optical network (PON) section of the network, where downstream capacity is twice the upstream capacity. In the following, we therefore limit our analysis to the downstream portion of traffic, since upstream traffic demands will automatically be met if the network can support the downstream traffic.

Starting from the average bit rate per subscriber (Table I), to account for traffic fluctuation, we take the provisioned bit rate per subscriber at busy hour to be 16 times larger: we apply a factor 2x for the peak-to-average ratio in a diurnal cycle, 2x to account any occasional larger volumes, and 4x to ensure an upgrade of aggregation capacity is only needed every couple of years (4x is a factor that is often used in practice by telecom operators to account for this).

¹Traffic volumes for fixed access and residential fixed access were estimated by direct fractional interpolation using global and regional subtotals.

²We differentiate between Internet traffic (with sub-categories web services, file sharing, gaming, VoIP, and video) and managed IP traffic (mainly video, which is chiefly downstream traffic) to determine the DS/US ratio.

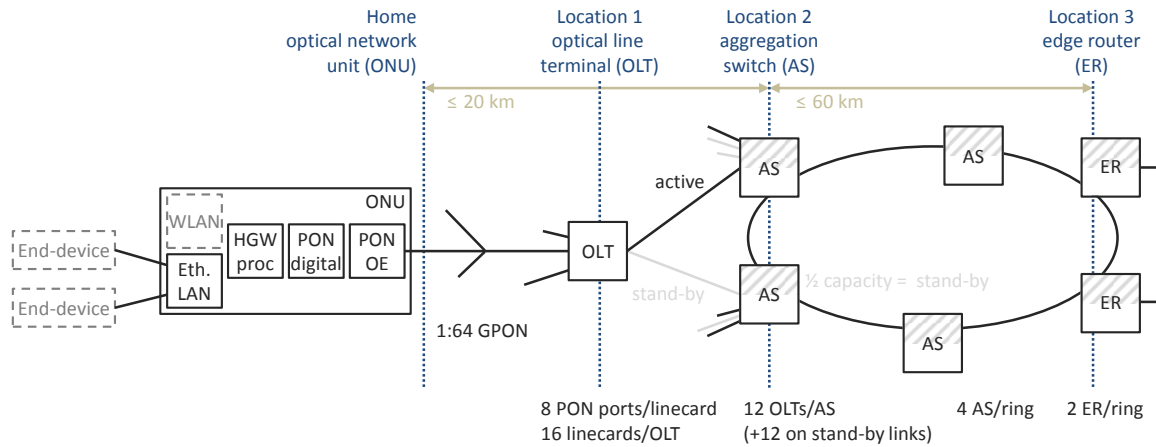


Fig. 2. Baseline and BAU network architecture

TABLE I
TRAFFIC AND SUBSCRIBER PROJECTIONS FOR RESIDENTIAL FIXED ACCESS IN GROUP 1 COUNTRIES

Year	2010	2020
Total (DS+US) traffic	11 EB/month	88 EB/month
Number of subscribers	245 million	281 million
Average total (DS+US) bit rate per subscriber	138 kb/s	955 kb/s
Average DS/US ratio	79/21	83/17
Average DS bit rate per subscriber	109 kb/s	796 kb/s
Provisioned bit rate per subscriber at busy hour	1.75 Mb/s	12.73 Mb/s

is dimensioned such that the total ring throughput can be supported in case the other ER fails.

To dimension the network nodes, we start from the provisioned bit rate per subscriber at the ONU (Table I). In each subsequent aggregation stage in the network, the traffic load is multiplied by the total number of subscribers served by that node to obtain the provisioned throughput in Table II. The interfaces are chosen in such a way that they can support this throughput with minimal power consumption.

Table II also shows how we expect the configuration and interfaces to change by 2020 in a BAU scenario, to accommodate the growing number of subscribers and traffic throughput.

C. Baseline and BAU network

The access network architecture for the baseline and BAU scenario is shown in Figure 2. As baseline residential access technology in 2010, we consider gigabit-capable passive optical network (GPON) with 2.5/1.25 Gb/s (DS/US) capacity as this was the most energy-efficient commercially deployed technology at the start of GreenTouch. In the BAU scenario we assume this technology will still be used in 2020, since bit rates per subscriber will not exceed GPON capacity.

The ONUs³ are connected to the OLT through a 1:64 split PON. We assume a filling rate of 50% in 2010 (32 subscribers per PON on average), which increases to 57.32% in 2020 (36.7 subscribers per PON on average), proportionally with the growth in number of subscribers (Table I). The traffic from twelve OLTs⁴ is aggregated on a single connection to an AS, with a second stand-by link to another AS as back-up. Every AS is a Layer 2 (L2) Ethernet switch with virtual local area network (VLAN) and multiprotocol label switching (MPLS) capability. Network resiliency is further improved by use of a ring topology encompassing 4 ASs and 2 ERs with redundant capacity. The ERs are Layer 3 (L3) service routers (also BRAS in older architectures) that form the connection to the core network. Under normal operation, the load is shared and each ER supports half the ring throughput. But each ER

III. GREENTOUCH TECHNOLOGIES AND ARCHITECTURE

The key technologies that enable drastic energy savings compared to the BAU scenario for 2020 are introduced in this section. Since the focus of this work is on the Green Meter calculation method for energy savings, we will limit our description of the enabling technologies to high-level concepts. The corresponding power-saving factors will be given in Section IV. Technical implementation details can be found in the GreenTouch white paper on fixed access [9] and in the references cited below.

A. Disruptive technologies

1) *Cascaded bit-interleaved PON*: Though bit rates per subscriber will not exceed GPON capacity by 2020, higher-capacity PONs are still worth considering because they allow OLT equipment to be shared between more subscribers per PON, resulting in power savings at the OLT. On the other hand, when optical access networks start offering higher data rates up to 40 Gb/s DS on a single PON, the fast processing of information in short time-slots at a very high data rate becomes one of the main power consumption drivers in the ONU. bit-interleaved PON (Bi-PON) is a new protocol that allows extracting the relevant bits for the ONU immediately behind the clock and data recovery [10], so that further processing is done at the lower user rate instead of the aggregate line rate. By arranging the transmitting data streams destined for

³Since the ONU power consumption is dominant, we further break it down into the sub-functions shown in the figure. For details, see Section IV-A.

⁴We use the term OLT to refer to one OLT rack.

TABLE II
 NODE DIMENSIONING FOR RESIDENTIAL ACCESS IN 2010 BASELINE NETWORK, AND EXPECTED CHANGES BY 2020 IN BAU SCENARIO

		ONU	OLT	Aggregation switch (AS)	Edge router (ER)
Configuration	2010	-	50% filling of 1:64 PON, 8 ports per linecard, 16 linecards. (1+1) uplinks to ASs	12 active and 12 stand-by OLT uplinks. (1+1) links to ERs	2 ER per 4 ASs in ring. (1+1) capacity
	2020	-	57.32% filling of 1:64 PON (ports, cards, uplinks same as 2010)	(same as 2010)	(same as 2010)
# subscribers (avg)	2010	1	4096	49152	98304
	2020	1	4695.3	56344	112688
Provisioned throughput	2010	1.75 Mb/s	7.2 Gb/s	86 Gb/s	(1+1)x172 Gb/s
	2020	12.73 Mb/s	60 Gb/s	717 Gb/s	(1+1)x1.43 Tb/s
Interfaces	2010	2xGbE LAN over copper Subscriber side: Network side: GPON (2.5/1.25 Gb/s DS/US)	GPON ports (2.5/1.25 Gb/s)	(1+1) x 12 x 10 Gb/s	(1+1) x 2 x 100 Gb/s
			(1+1) x 10 Gb/s	(1+1) x 100 Gb/s	(2+2) x 100 Gb/s
	2020	(same as 2010)	(same as 2010)	(1+1) x 12 x (2x40) Gb/s	(1+1) x 2 x (8x100) Gb/s
			(1+1) x (2x40) Gb/s	(1+1) x (8x100) Gb/s	(15+14) x 100 Gb/s

different ONUs in bitwise interleaving fashion⁵, the Bi-PON protocol enables the ONUs to sample data in the physical domain. All subsequent processing at the ONU can then be operated at the lower clock rate, thus resulting in power savings [11].

Moreover, the concept has been extended to multiple cascaded levels, namely a CBI-PON [12], where lower level Bi-PONs are connected to their upper level network through CBI *repeaters*: the frame structure is designed such that these intermediate nodes can perform a simple down-sampling function to efficiently extract only the portion of data that is relevant to the nodes subtending that repeater. The lower level Bi-PON supports a variety of DS line rates which can be equal to 1/4, 1/8, 1/16 or 1/32 of its upper level Bi-PON. The introduction of CBI results in a long reach access network and even better sharing of the OLT in comparison with regular Bi-PON.

2) *Virtual home gateway*: In the baseline network, home gateway (HGW) service functions (forwarding, firewalling, network address translation, dynamic host configuration protocol server, and administration interface) are physically located at dedicated resources at every ONU. In the GT 2020 scenario the HGW at the user premise is replaced by a quasi-passive device without special features. The resource intensive HGW services are pulled to servers that are co-located with the ER. The functions are virtualized into *containers* on the central servers, exploiting scaling and sharing of resources to realize energy savings [13]. GreenTouch demonstrated that a single server can host up to one thousand virtual home gateways [14]. This approach still provides isolation between users, and the provider can take advantage of consolidation for easier future expansion of gateway functionality to advanced services such as video storage or console gaming, while keeping the ONU simple, low-power and reliable.

⁵Upstream rates are typically lower (1/2 or 1/4) than downstream, therefore bit-interleaving is only applied downstream; upstream transmission remains a simple time-slot based transfer.

3) *PtP transceiver*: In the GreenTouch architecture, in-home copper links are replaced by fiber links. In particular, the traditional Gigabit Ethernet (GbE) local area network (LAN) interfaces are replaced by low power PtP optical transceivers. Conventional PtP optical transceivers operate continuously at a high and fixed optical power and the electronic-to-optical signal conversion efficiency is relatively low [15]. GreenTouch researchers have completely redesigned the transceiver and custom-built an application-specific integrated circuit (ASIC) prototype that minimizes the circuit power consumption for a target data rate up to 1 Gb/s. The savings are enabled by system simplification, better system integration, optimizing the transmitter circuitry and signaling, and adapting the transmitter power based on the link distance [16], [17].

4) *low-power optics and electronics (LPOE) – Innovations in optics and electronics*: Progress in optical components and electronic circuit technology can reduce power to a fraction 0.75 and 0.33 respectively beyond BAU trends, if special attention is paid to energy efficiency in hardware design. Further, improved PON optoelectronics (OEs) would allow elimination of the limiting amplifier (LA) in the ONU, thereby also eliminating its power consumption. In this work, we group these savings under the term LPOE.

5) *Sleep modes*: Power consumption can be reduced by switching components from the full power active state to a low power sleep state depending on the traffic load and redundancy requirement. Cyclic sleep mode [18] is used in the access (cf. ITU-T G.987.3) and Ethernet LAN (cf. IEEE802.3az) interfaces. In the PON based access, where a point-to-multipoint topology applies, cyclic sleep mode is applicable mostly at the ONU interface; since the OLT interface is shared, the savings at the OLT are smaller. Where a point-to-point topology applies, as is the case in PtP Ethernet LAN links, cyclic sleep mode is applicable symmetrically at both ends of the link leading to larger savings. At the ER, we account for turning stand-by elements (provisioned for redundancy) to a sleep state such that a quick turn on is ensured.

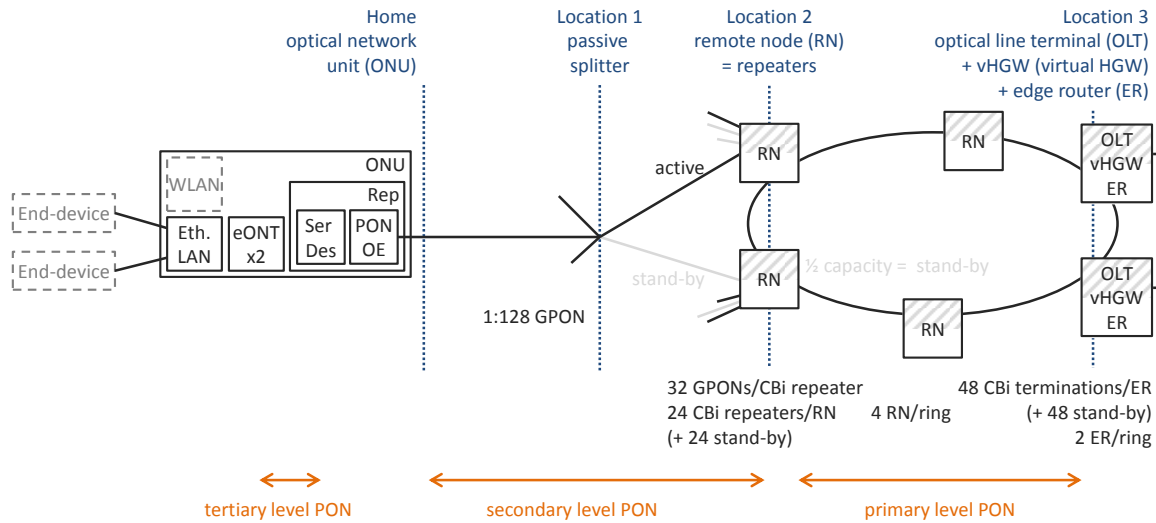


Fig. 3. GreenTouch network architecture

TABLE III
NODE DIMENSIONING FOR RESIDENTIAL ACCESS IN 2020 GREENTOUCH NETWORK

	ONU	Remote node (RN)	OLT + vHGW + ER
Configuration (avg)	-	57.32% filling of 1:128 PON 32 ports per repeater (24+24) repeaters (24+24) uplinks to ERs	4 CBI-PON terminations per linecard (12+12) linecards per ER 2 ER per 4 RNs in ring
# subscribers (avg)	1	56,344.10	112,688
Provisioned throughput	12.73 Mb/s	717 Gb/s	(1+1) x 1.43 Tb/s
Interfaces	2xGbE LAN over fiber GPON (2.5/1.25 Gb/s DS/US)	Subscriber side: GPON ports (2.5/1.25 Gb/s DS/US) Network side: (24+24) x 40 Gb/s	Subscriber side: (48+48) x 40 Gb/s Network side: (15+14) x 100 Gb/s

B. Network architecture integrating all GreenTouch solutions

The GreenTouch residential access network for 2020 is shown in Figure 3. As the introduction of CBI allows an extension of PON reach, the OLT is moved to the ER location (along with the virtualized HGW functionality), and the AS is replaced by a remote node (RN) with simple CBI repeaters. The repeaters in the RN downsample the CBI signal coming from the ER (primary level PON) to divide it between 32 GPONs (secondary level PON). The GPON signal is downsampled a second time in the ONU, where the relevant bits for two LAN interfaces are selected and directed to the appropriate end-ONT (eONT) (tertiary level PON). The node dimensioning for this architecture is detailed in Table III.

The tertiary level PON (in-home) supports 1.25 Gb/s DS and 625 Mb/s US. The eONT functions within the ONU terminate the PON extracting the traffic for the respective LAN interfaces. The repeater function of the ONU eliminates the need for a switching function within the ONU, since the bits are interleaved so that the repeater automatically directs them to the eONT corresponding to the correct LAN interface.

The CBI repeater in the remote node has a standard GPON OLT optical front-end to the subscriber side, so the secondary level PON supports 2.5 Gb/s DS and 1.25 Gb/s US. We assume that 1:128 split in each GPON is possible since this is regular OLT optics state of the art as of 2017 (year of assumed introduction). The power consumption of the GPON

OLT remains, but is moved higher up in the network and integrated in the ER. clock and data recovery (CDR) and serializer/deserializer (SerDes) are shared between 32xGPON.

To the metro ring side, the CBI repeater in the remote node has a 40G transceiver. The 40G link in the metro ring is oversubscribed by 2x on the downstream side when considering the GPON downstream capacity of 32x2.5G, but a dynamic bandwidth (BW) allocation by the bit-interleaving scheduler allows to manage all DS subscriber traffic since the sustained user throughput is only about 30 Gb/s.

The load in the metro ring is still shared between two ERs, where each ER supports half the throughput (1.43 Tb/s) under normal operation, but each ER is dimensioned to support the total throughput (2.87 Tb/s) in the event that one of them fails. Under normal operation, the power consumed by the redundant network elements is reduced by switching to a low power stand-by state consuming 20% of the active power in order to ensure quick turn on when needed.

The ER chassis features a 40G transceiver into each PtP link which connects to the metro ring CBI repeater; the CBI-PON primary level (Metro/Edge PON) supports asymmetrical rates of 40 Gb/s DS and 10 Gb/s US. In addition, the OLT electronics for processing the GPON traffic are included in the ER power calculation. No amplification is needed on <60 km links at 40G (18 dB fiber loss), which should cover most deployments. The ER does not have user side blades because

PON OLT blades are directly integrated in the ER chassis.

IV. THE GREEN METER MODEL

Implementing green technologies affects different parts of the network to a different extent, hence calculating the overall savings can not be done through a straightforward multiplication of saving factors. The approach we propose in the Green Meter is to break the system down into power consumption components and determine the saving factors for individual components, after which the total power is obtained by calculating the sum of products.

We apply this approach to the optical access network in Table IV. In the following, we start by introducing the baseline power consumption values and general calculation method. Next, we explain how we obtain each factor in the table. References are included where available; the other factors are own estimates based on typical values or confidential sources.

A. Baseline power of system components

The top rows of Table IV show how we break the nodes down into components. The model is most detailed for the dominant contributors to power consumption. All power values include power supply inefficiency for all nodes (90% AC/DC and 90% DC/DC conversion); cooling overhead for OLT, AS, and ER equipment (50% overhead in 2010); and redundant elements for resiliency as indicated by the $(X+X)$ terms in Table II and Table III (where X represents a number of devices).

The ONU is broken down into the following sub-functions:

- optoelectronic (OE) conversion of signals
 - optics (265.81 mW): accounting for uncooled distributed feedback (DFB) directly modulated laser (DML) at 1.25G (3.3 V supply to laser driver, 15 mA biasing current, and 50 mA modulation current) and PIN diode
 - electronics (391.19 mW): including transimpedance amplifier (TIA) at 2.5G [19], burst-mode (BM) control and monitor part [20], and LA at 1.25G
- Digital protocol processing in a system-on-chip (SoC) (1.481 W [21])
- Integrated HGW processor to handle forwarding, fire-walling, network address translation, dynamic host configuration protocol server, and administration interface (1.9 W, estimate derived from [22] and consumption of other ONU parts)
- Two wireline GbE LAN interfaces to connect end devices (1.975 W [22])

Note that wireless local area network (WLAN) interfaces and end-devices are not relevant in the comparison of fixed access technologies and hence excluded in our analysis.

At the OLT, power estimates are made for one OLT port (serving 32 subscribers in 2010). We consider the following sub-functions:

- OE conversion of the signals from the PON:
 - optics (440.72 mW): accounting for uncooled DFB DML at 2.5G (3.3 V supply to laser driver, 17 mA

biasing current, and 55 mA modulation current) and PIN diode

- electronics (1117.8 mW): including TIA at 1.25G [23], laser driver continuous wave (CW) power control, and BM LA at 1.25G (scaled down from [24])

- Digital processing (11 W): estimate derived from [22], subtracting consumption of other OLT parts. 28% of this power is throughput-dependent (dynamic); the remaining 72% is constant under varying traffic loads (static).

We further consider power consumption in the AS (5.9 kW) and ER (7.8 kW): the power per node is estimated by summing values for chassis, fabric, input/output (IO) modules, and blades to support the calculated throughput and interfaces. Since these nodes contribute relatively little to the overall power per subscriber, we do not break them down into components.

All power consumption values above are calculated on a per-node basis. To obtain the power per subscriber (sub), the power per node is divided by the number of subscribers per node, which can be derived from Table II.

$$P_{sub} = \frac{P_{node}}{\#subs_{node}} \quad (1)$$

Note that at the OLT, we consider each termination port of a single PON to be a “node”, so $\#subs_{OLT,2010} = 32$ (instead of 4096, the number of subscribers per OLT rack given in Table II).

B. Future power estimates: calculation method

The power per node $P_{K,C}$ of a component C ($C =$ one of the variable names defined in the column headers of Table IV) in 2020 when K ($1 \leq K \leq 9$) energy-saving techniques are applied, is obtained by multiplying the baseline power of that component in 2010 ($P_{0,C}$) with the appropriate traffic growth factor g_C (see next section) and the appropriate energy-saving factors $f_{k,C}$ for technologies $k = 1..K$.

$$P_{K,C} = P_{0,C} * g_C * \prod_{k=1..K} f_{k,C} \quad (2)$$

To obtain the 2020 BAU estimates, the four first techniques are taken into account ($K = 4$). For example, substituting the values for OE optics in the OLT (column six in Table IV), we get $330.54 \text{ mW} = 440.7 \text{ mW} * 1.00 * 1.00 * 1.00 * 1.00 * 0.75$.

The power per subscriber for a component C in 2020 ($S_{K,C}$) is obtained by applying a similar formula to the baseline power per subscriber of that component ($S_{0,C}$), but including the appropriate “number of subscribers” factors $s_{l,C}$, indicated in grey in Table IV, to account for changes in the number of subscribers per node.

$$S_{K,C} = S_{0,C} * g_C * \prod_{k=1..K} f_{k,C} * \prod_{l=1..L} s_{l,C} \quad (3)$$

with

$$L = \begin{cases} 1, & \text{if } 1 \leq K \leq 4 \\ 2, & \text{if } K \geq 5 \end{cases} \quad (4)$$

TABLE IV

GREEN METER POWER MODEL AND POWER-SAVING FACTORS. ENERGY-SAVING FACTORS CAN BE MULTIPLIED VERTICALLY, FROM TOP TO BOTTOM, TO OBTAIN POWER PER NODE IN FUTURE SCENARIOS. INCLUDE FACTORS IN GRAY TO CALCULATE POWER/SUBSCRIBER. EXAMPLE: IN COLUMN EIGHT, $1117.8 \text{ mW} * 0.37 * 1 * 0.80 * 0.75 = 248.15 \text{ mW}$, AND $248.15 \text{ mW} * 0.889 * 1 * \dots * 1 = 220.57 \text{ mW}$. INTERMEDIATE SCENARIOS CAN ALSO BE CALCULATED BY MULTIPLYING ONLY A SELECTION OF FACTORS (E.G. APPLYING ONLY MOORE'S LAW AND POWER SHEDDING IN COLUMN EIGHT RETURNS $1117.8 \text{ mW} * 0.37 = 414 \text{ mW}$), BUT ROWS CANNOT BE SKIPPED, AS INTRODUCING ONE TECHNOLOGY MAY INFLUENCE THE SAVING FACTOR OF THE NEXT.

Node (baseline)	ONU					OLT port (serves 1 PON)				AS	ER
Node components	PON OE optics	PON OE electronics	Digital SoC	HGW processing	2xGbE LAN	OE optics	OE electronics	Digital: dynamic	Digital: static	(all)	(all)
Column labels	<i>HO</i>	<i>HE</i>	<i>HD</i>	<i>HG</i>	<i>HL</i>	<i>TO</i>	<i>TE</i>	<i>TD</i>	<i>TS</i>	<i>AS</i>	<i>ER</i>
Power: 2010 baseline											
P_0 (mW/node)	265.81	391.19	1481.0	1900.0	1975.3	440.72	1117.8	4183.6	1.076E+04	5.926E+06	7.778E+06
S_0 (mW/subscriber)	265.81	391.19	1481.0	1900.0	1975.3	13.77	34.93	130.74	336.18	120.56	79.12
Power increase due to traffic growth by 2020											
Growth factor g	1.00	1.00	1.00	1.00	1.00	1.00	1.00	7.93	1.00	[in $f_{1,2,3}$]	[in $f_{1,2,3}$]
#subs factor s_1	1.000 ^a	0.872 ^a	0.872 ^a	0.872 ^a	0.872 ^a	0.872 ^a	0.872 ^a				
Energy-saving factors: BAU											
f_1 Moore's Law	1.000	0.370	0.261	0.261	0.261	1.000	0.370	0.261	0.261	2.25	2.38
f_2 Power shedding	1.000	1.000	1.000	0.475	0.475	1.000	1.000	1.000	1.000		
f_3 Efficient HW design	1.000	0.800	0.800	0.800	0.800	1.000	0.800	0.800	0.800	0.750	0.750
f_4 Efficient cooling	1.000	1.000	1.000	1.000	1.000	0.750	0.750	0.750	0.750	0.750	0.750
Power: 2020 BAU											
P_4 (mW/node)	265.81	115.79	309.50	188.60	196.08	330.54	248.15	5201.2	1686.1	1.000E+07	1.389E+07
S_4 (mW/subscriber)	265.81	115.79	309.50	188.60	196.08	9.01	6.76	141.79	45.97	177.48	123.25
Energy-saving factors: GT											
f_5 CBI-PON	1.000	1.000	0.281	0.799	1.000	0.889 ^b	0.889 ^b	2.200 ^c	1.100 ^c	0.00056 ^d	0.533 ^e
#subs factor s_2	1.000 ^a	0.500 ^a	0.500 ^a	0.500 ^a	0.500 ^a	24.000 ^a	1.000 ^a				
f_6 vHGW	1.000	1.000	1.000	0.101 ^f	1.000	1.000	1.000	1.000	1.000	1.000	1.000
f_7 PtP TRx	1.000	1.000	1.000	1.000	0.269	1.000	1.000	1.000	1.000	1.000	1.000
f_8 LPOE	0.750	0.686	0.330	0.330	0.977	0.750	1.000	0.330	0.330	0.940	0.998
f_9 Sleep mode	0.0761	0.371	0.476	1.000	0.354	1.000	1.000	0.800	0.800	1.000	0.662
Power: 2020 GT											
P_9 (mW/node)	15.18	29.48	13.67	5.00	18.25	220.36	220.57	3020.9	489.6	5244.6	4.891E+06
S_9 (mW/subscriber)	15.18	29.48	13.67	5.00	18.25	3.00	3.01	41.18	6.67	2.23	43.41
Node (GT)	ONU			ER	ONU	RN		ER	RN		ER

^a Factor due to change in number of subscribers per node. Only applies to power/subscriber, not to power/node.

^b OLT OE components are relocated to RN (long reach PON).

^c OLT digital functions are moved to ER location (long reach PON).

^d AS functionality is replaced by a simple repeater in the RN.

^e CBI termination is added to ER functionality.

^f HGW functionality is moved to ER location.

For example, there are 36.68 subscribers per PON in the 2020 BAU scenario ($K = 4$) where there used to be 32, so OE optics power per subscriber becomes $9.01 \text{ mW} = 13.77 \text{ mW} * 1.00 * 0.872 * 1.00 * 1.00 * 1.00 * 0.75$ (indeed, $9.01 \text{ mW} = 330.54 \text{ mW} / 36.68$). Arguably power per subscriber is a more interesting metric than power per node in this context. When the number of subscribers per node changes, the power per node in Table IV does not reflect how many nodes are needed and thus, how much the network as a whole will consume. Nevertheless, we chose to include both, in order to provide more clarity on how the saving factors were obtained.

To obtain 2020 GT estimates, the calculations are performed for $K = 9$. Intermediate scenarios can also be evaluated ($4 \leq K \leq 9$), as long as no technologies are skipped. This

condition follows from the fact that the order of introduction of technologies can impact saving factors: for example, introducing CBI first reduces the potential for sleep mode, so the saving factor for sleep mode in the table is only correct in a scenario where CBI is already introduced. Although changing the order of introduction can change the saving factors for individual technologies, the overall savings in the 2020 GT scenario, which incorporates all technologies, will remain the same regardless of the order of introduction.

C. Power change due to traffic and subscriber growth

The goal of the calculations in Table IV is to obtain power estimates for 2020 in a BAU and GT scenario, taking into account saving factors from various technological advances.

But before any saving factors are applied, we need to consider the impact of traffic growth between 2010 and 2020 on power consumption of the baseline scenario. This is done through the *traffic growth factor* g_C in Table IV. As we already mentioned in Section II-C, GPON can still be used in the last mile. Since the baseline ONU power is independent of traffic throughput, it will remain constant despite the growth in throughput per subscriber, so $g_{ONU} = 1$. In the OLT, the same is true for all components except for the dynamic portion of digital processing, which increases proportionately with the traffic load per PON. Since the number of PONs does not change between 2010 and 2020 BAU, this is equivalent to the total traffic growth. If we call the power taking into account only traffic growth P_g , we get:

$$P_{g,TD} = P_{0,TD} * \frac{T_{2020}}{T_{2010}} = P_{0,TD} * 7.93 \quad (5)$$

where T_y is the total⁶ traffic load in year y , taken from the first row in Table I. For the AS and ER a simplified approach is used: there is no separate traffic growth factor for these nodes; instead, we assume that the power consumption stays flat for an evolution to the next generation of technology with 4 times better throughput, thanks to a higher level of ASIC integration and Moore's law (introduced in the next section). This evolution is lumped together in a single factor in Table IV along with the remaining effect of traffic growth on power consumption (for the relevant components), leading to a 2.25-fold increase in power per AS and a 2.38-fold increase in power per RN.

The BAU scenario takes into account a growing take up rate in the PON to serve the growing number of subscribers (from 32 to 36.68 subscribers per PON, cf. Table II). This results in better equipment sharing and, as a consequence, a lower power per subscriber. This is reflected by the first *#subs factor* in Table IV for OLT, AS and ER:

$$\begin{aligned} s_{1,\{OLT,AS,ER\}} &= \frac{\text{\#subs using component } C \text{ in 2010}}{\text{\#subs using component } C \text{ in 2020}} \\ &= \frac{32}{36.68} = 0.872 \end{aligned} \quad (6)$$

At the ONU, the #subs factor is one (no change), since there is one subscriber per ONU in all scenarios.

D. BAU saving factors

The first factor we apply follows from *Moore's law*, which is the observation that over the history of computing hardware, circuit integration density has doubled approximately every two years. This miniaturization reduces the driving voltage of electronic circuits, which in turn has an impact on power dissipation. Moore's law is applied to all electronics but not to optics (lasers and photodetectors). The saving factor depends on the type of electronics: digital or analog.

For digital electronics, we distinguish between logic and IO. The scaling of logic has been described in [25] to follow an 8x energy per flop improvement in 10 years, equivalent to

dividing the power by a factor 1.22 annually. For IO, the work in [26] indicates that off chip interconnect should scale with technology node size, which scales at about 10 percent per year, dividing power dissipation by 1.1 annually. Combining these two parts, with logic and IO each contributing about half of the digital electronics power, we get:

$$\begin{aligned} P_{1,dig} &= P_{g,dig} * \left(0.5 * (1/1.22)^{10} + 0.5 * (1/1.1)^{10} \right) \\ &= P_{g,dig} * 0.261 \end{aligned} \quad (7)$$

with

$$dig \in \{HD, HG, HL, TD, TS\} \quad (8)$$

For analog electronics, the power scales linearly with the driving voltage. Since digital logic power scales with the square of the driving voltage, we apply the square root of the annual improvement factor from digital logic here:

$$\begin{aligned} P_{1,\{HE,TE\}} &= P_{g,\{HE,TE\}} * \left(1/\sqrt{1.22} \right)^{10} \\ &= P_{g,\{HE,TE\}} * 0.370 \end{aligned} \quad (9)$$

Power shedding is characterized by powering off or reducing power to non-essential functions and services in the ONU while maintaining a fully operational optical link [27]. It is applied to the GbE interface and HGW processing. Power shedding techniques were already available in 2010, but they were only used in the event of a mains power failure [28]. In order to reduce network energy consumption, the feature is extended to power savings during idle periods. If we assume a component uses about one tenth of the active power in power-shed state, and the ONU is used 10 hours a day on average, we get

$$\begin{aligned} P_{2,ps} &= P_{1,ps} * 10/24 + P_{1,ps} * 0.1 * 14/24 \\ &= P_{1,ps} * 0.475 \end{aligned} \quad (10)$$

with

$$ps \in \{HG, HL\} \quad (11)$$

Further, we predict *energy efficient hardware (HW) design* will cut back power for all electronic components by another twenty percent:

$$P_{3,el} = P_{2,el} * 0.80 \quad (12)$$

with

$$el \in \{HE, HD, HG, HL, TE, TD, TS\} \quad (13)$$

Recent years have also shown a trend of more *efficient cooling* techniques being used in data centers and the buildings that house telecommunication equipment (so-called central offices) [29]. We expect the cooling overhead to drop from 50% to 12.5% between 2010 and 2020:

$$\begin{aligned} P_{4,\{OLT,AS,ER\}} &= P_{3,\{OLT,AS,ER\}} / 1.50 * 1.125 \\ &= P_{3,\{OLT,AS,ER\}} * 0.75 \end{aligned} \quad (14)$$

E. GreenTouch saving factors

Starting from the BAU scenario, more radical approaches can be introduced to achieve even better energy efficiency in the GT 2020 scenario.

⁶Note that dynamic power consumption scales with total traffic requirements (US + DS), whereas capacity requirements are dimensioned for the most demanding traffic direction (DS).

1) *Cascaded Bi-PON*: reduces the energy need for digital processing in the ONU. The 2.5G repeater consumes 188.27 mW, and the two 1G eONTs 2*114.20 mW (values from power estimation tools applied to the chip design for CBI [30]). Because these values are not yet taking into account BAU improvements, the saving factor is obtained by dividing the sum of the aforementioned values by the baseline power for digital processing (1481.0 mW)

$$P_{5,HD} = P_{4,HD} * \frac{416.67 \text{ mW}}{1481.0 \text{ mW}} = P_{4,HD} * 0.281 \quad (15)$$

Secondly, the introduction of CBI makes the switching function in the ONU obsolete. When switching power (381.48 mW in the baseline) is subtracted from HGW processing power, we get

$$\begin{aligned} P_{5,HG} &= P_{4,HG} * \frac{1900.0 \text{ mW} - 381.48 \text{ mW}}{1900.0 \text{ mW}} \\ &= P_{4,HG} * 0.799 \end{aligned} \quad (16)$$

As outlined in the architecture description in Section III-B, some of the network equipment is replaced and/or relocated when CBI is introduced. The OLT is replaced by a passive splitter and the OE conversion of the signals from the PON is relocated to the RN which, contrary to the OLT, is uncooled. This means the cooling overhead (12.5 percent in 2020 – we consider the factor for 2020 because energy efficient cooling was already incorporated in the BAU factors) is no longer required:

$$P_{5,\{TO,TE\}} = P_{4,\{TO,TE\}}/1.125 = P_{4,\{TO,TE\}} * 0.889 \quad (17)$$

The OLT digital processing is moved to the ER location (which is cooled, so the savings factor from (17) does not apply here) and an overhead factor 1.1x is applied to implement the interleaving function. The number of subscribers per OLT port doubles when CBI is introduced, since the split ratio is doubled with respect to the BAU scenario. Consequently, the dynamic part of the digital processing power is doubled (in terms of power per subscriber, this will be compensated by the #subs factor in equation (20)).

$$P_{5,TD} = P_{4,TD} * 1.1 * 2 \quad (18)$$

The static part is independent of throughput and becomes

$$P_{5,TS} = P_{4,TS} * 1.1 \quad (19)$$

The doubling of the number of subscribers per OLT port is taken into account in the power/subscriber calculation by including the #subs factor for all OLT components:

$$\begin{aligned} s_{2,OLT} &= \frac{\#subs \text{ using OLT port before CBI}}{\#subs \text{ using OLT port after CBI}} \\ &= \frac{0.5732 * 64}{0.5732 * 128} \\ &= 0.500 \end{aligned} \quad (20)$$

The AS is replaced by a simple RN containing multiple CBI repeaters. Each repeater consumes: 1349.38 mW in 40G transceiver (TRx) optics (externally modulated laser (EML) [31], avalanche photodiode (APD) and TIA),

968.85 mW in 40G TRx electronics (EML driver + LA [32], [33]; already taking into account Moore's law for analog electronics, cf. (9)), and 3263.76 mW for digital processing of 32 GPONs bundled in each repeater (values from power estimation tools applied to the chip design for CBI [30]; already taking into account Moore's law for digital electronics, cf. (7)). The power calculation becomes

$$\begin{aligned} P_{5,AS} &= P_{4,AS} * \frac{1349.38 + 968.85 + 3263.76 \text{ mW}}{1.000 * 10^7 \text{ mW}} \\ &= P_{4,AS} * 5.6 * 10^{-4} \end{aligned} \quad (21)$$

where it should be noted that the label *AS* from here on denotes the repeater (REP). Note that the number of subscribers per REP is much smaller than the number of subscribers per former AS, resulting in a high #subs factor:

$$\begin{aligned} s_{2,AS} &= \frac{\#subs \text{ connected to AS before CBI}}{\#subs \text{ connected to CBI REP}} \\ &= \frac{56344}{32 * (0.5732 * 128)} \\ &= 24 \end{aligned} \quad (22)$$

This partly cancels the savings in (21), but combined, it still results in a 98.7 percent reduction of this node's power per subscriber (combined factor = 0.013).

The ER is replaced by a more energy-efficient model than the BAU version, now consuming only 7.22 kW to route traffic from the same number of subscribers (#subs factor = 1.000). The power of the CBI termination, which is co-located with the ER, is added. Termination of a single CBI PON requires 3901.42 mW: 1518.06 mW in 40G TRx optics and 1089.96 mW in electronics (identical to the 40G TRx in RN but x1.125 to include cooling), and 1293.41 mW for the SerDes with CDR and electronic dispersion compensation (EDC) (power from [34] scaled up to 40G, taking into account cooling and Moore's law for digital electronics, cf. (7)). Since there are 48 CBI terminations in each ER node, the saving factor becomes:

$$\begin{aligned} P_{5,ER} &= P_{4,ER} * \frac{7.22 * 10^6 + 48 * 3901.42 \text{ mW}}{1.389 * 10^7 \text{ mW}} \\ &= P_{4,ER} * \frac{7.41 * 10^6}{1.389 * 10^7 \text{ mW}} \\ &= P_{4,ER} * 0.533 \end{aligned} \quad (23)$$

2) *Virtual HGW*: GreenTouch demonstrated that 1000 virtual home gateways can be hosted on a single server consuming 203.7 W, or 203.7 mW per subscriber. With efficient cooling, this becomes 152.8 mW per subscriber in 2020. Compared to equivalent functions in the baseline network (excluding switching in line with (16)), this technology provides a saving factor

$$\begin{aligned} P_{6,HG} &= P_{5,HG} * \frac{152.8 \text{ mW}}{1900.0 \text{ mW} - 381.48 \text{ mW}} \\ &= P_{5,HG} * 0.101 \end{aligned} \quad (24)$$

at the HGW processing sub-component. This factor is applied on top of BAU energy-saving factors, since these factors remain applicable when functionality is moved to the server.

3) *Redesigned PtP TRx in LAN*: The copper LAN interfaces are replaced by new PtP TRxs. The power consumption of one such interface is the sum of three contributions: 5.1 mW in optics (PIN diode + laser), 3.6 mW in analog electronics (TIA + LA + driver CW), and 46.8 mW in the SerDes. These values from [35] already account for Moore's law, but we still need to include power shedding. Therefore we multiply the total power per transceiver by 0.475, resulting in a power consumption of 26.4 mW per redesigned PtP TRx. The saving factor in Table IV is obtained by dividing the power for two optical interfaces by that of the two copper interfaces in the BAU scenario:

$$\begin{aligned} P_{7,HL} &= P_{6,HL} * \frac{2 * (5.1 + 3.6 + 46.8) * 0.475 \text{ mW}}{196.06 \text{ mW}} \\ &= P_{6,HL} * 0.269 \end{aligned} \quad (25)$$

4) *Low power optics and electronics*: Progress in optical components and electronic circuit technology beyond BAU trends, and improved PON OE will further reduce power at the applicable sub-components. These savings are grouped under the name LPOE in Table IV. The individual factors are obtained as follows.

Progress in optical components beyond BAU trends results in 25% savings, which apply directly to PON and OLT optics:

$$P_{8,\{HO,TO\}} = P_{7,\{HO,TO\}} * 0.75 \quad (26)$$

The 25 percent savings also apply to the optical part of the two LAN interfaces, which, as shown in (25), is (5.1 mW*0.475) per transceiver. Since the total power per transceiver is 26.4 mW, this translates to:

$$\begin{aligned} P_{8,HL} &= P_{7,HL} * \frac{(26.4 - 0.25 * 5.1 * 0.475) \text{ mW}}{26.4 \text{ mW}} \\ &= P_{7,HL} * 0.977 \end{aligned} \quad (27)$$

Similarly, for the optical part of the REP, from (21), we get:

$$\begin{aligned} P_{8,AS} &= P_{7,AS} * \frac{(5581.99 - 0.25 * 1349.38) \text{ mW}}{5581.99 \text{ mW}} \\ &= P_{7,AS} * 0.940 \end{aligned} \quad (28)$$

And for the optical part of the ER, from (23), we get:

$$\begin{aligned} P_{8,ER} &= P_{7,ER} * \frac{7.41 * 10^6 - 0.25 * 48 * 1518.06 \text{ mW}}{7.41 * 10^6 \text{ mW}} \\ &= P_{7,ER} * 0.998 \end{aligned} \quad (29)$$

Progress in electronic components beyond BAU trends results in 67% savings in electronics: ONU digital SoC, HGW processing, and OLT digital processing all fully benefit from these improvements, so we apply to all of these components:

$$P_{8,\{HD,HG,TD,TS\}} = P_{7,\{HD,HG,TD,TS\}} * 0.330 \quad (30)$$

Improved PON OE allows the elimination of the LA from PON OE electronics in the ONU. Extracting the LA power (123 mW*0.37*0.8 = baseline value from Section IV-A with Moore's law and efficient HW design applied) from the PON OE electronics power in the ONU (391.19 mW*0.37*0.8, same reasoning as for LA), we get:

$$\begin{aligned} P_{8,HE} &= P_{7,HE} * \frac{(391.19 - 123 \text{ mW}) * 0.37 * 0.8}{391.19 \text{ mW} * 0.37 * 0.8} \\ &= P_{7,HE} * 0.686 \end{aligned} \quad (31)$$

5) *Sleep modes*: Sleep modes are applied at the ONU, OLT, and ER.

a) *ONU sleep modes*: An adapted version of the probing-based cyclic sleep mechanism from [36] is applied at the LAN and PON interfaces in the ONU. Different sleep saving factors apply to optics, electronics and SoC; and within these components, different saving factors apply to the transmitter-side and receiver-side power. The sub-components that result from this division are listed in Table V. In this section, we start by deriving the individual saving factors of the sub-components (S_r and S_t for receiver and transmitter, respectively), before combining them to obtain the saving factors per component $f_{9,C}$ in Table IV.

To compute the power consumption of the LAN and PON receiver-side components in the ONU with sleep mode, we adapt the analysis in [36] with the following changes. The power consumption in idle and active state for receiver components are assumed to be the same. The probe state is, by definition, the same as the active state for the receiver. We also consider a wake-up time T_{rw} to turn on the receiver which applies for the transition from the sleep state to the probe (or active) state. The transition time T_u in [36] no longer applies as the probe and active states are the same. We can now adapt [36, Eqn. (8)] as follows. The average receiver-side power at the ONU with cyclic sleep mode is given by

$$\begin{aligned} P_{r,sleep} &= \frac{1}{\mathbb{E}[C]} \left((1 - e^{-\lambda T_t}) \left(\frac{1}{\lambda} - \frac{T_t e^{-\lambda T_t}}{1 - e^{-\lambda T_t}} \right) P_{ra} \right. \\ &\quad + e^{-\lambda T_t} T_t P_{ra} \\ &\quad + \mathbb{E}[\zeta] \left((T_s - 2T_{rw}) P_{rs} + T_p P_{ra} \right. \\ &\quad \left. \left. + 2T_{rw} \left(\frac{P_{rs} + P_{ra}}{2} \right) \right) \right) \\ &\quad + \mathbb{E}[B] P_{ra} \end{aligned} \quad (32)$$

where P_{ra} and P_{rs} denote the power consumption of the receiver component in active state and sleep state respectively, T_s and T_p are the time duration in sleep state and probe state for the cyclic sleep mode, and T_t is the trigger time, i.e., the duration of time in idle state after which cyclic sleep mode is initiated. The expressions for $\mathbb{E}[C]$, $\mathbb{E}[\zeta]$, and $\mathbb{E}[B]$ are accordingly calculated as in equations (7), (1), and (6) in [36]. Note that the computation in [36] applies to a standard time-division multiplexing (TDM)-PON. Since we use sleep mode on top of CBI where the traffic is bit-interleaved, the PON receiver needs to be on for a longer duration. We assume a 1.5x overhead on the power consumption applies due to this (this does not apply to the PtP LAN interface).

We take $T_t = 0.1 \text{ ms}$, $T_s = 10 \text{ ms}$ and, specifically in the PON receiver, $T_p = 250 \text{ } \mu\text{s}$, which is the time duration for two GPON frames, and in the LAN receiver, $T_p = 24 \text{ } \mu\text{s}$. The packet sizes are taken as 1500 bytes for simplicity. The average traffic rate is taken as 20 Mbps, from which the packet arrival rate λ in packets per second can be computed. The peak service rate is taken as 1 Gbps (reasoned by gigabit Ethernet), from which the packet service rate μ in packets

TABLE V
 ONU SLEEP MODE PARAMETERS

	α	S_r	S_t
PON OE optics	0.3%	0.152	0.076
PON OE electronics	52%	0.446	0.292
Digital SoC	50%	0.606	0.345
LAN optics	4%	0.081	0.071
LAN electronics	50%	0.282	0.275

per second can be computed. The sleep state power P_{rs} is taken as a percentage of the active state power P_{ra} based on the component (5% for optics, 25% for electronics, 30% for digital SoC). As a result, by normalizing $P_{ra} = 1$, we can essentially calculate the savings factor from sleep mode. The wake-up time T_{rw} is also based on the component (1 μ s for optics, 100 μ s for electronics, 1 *ms* for digital SoC).

To compute the power consumption of the PON transmitter components with sleep mode, we note that the transmitter is active only for the duration of transmission and is in sleep state otherwise. A small overhead (assumed 1.1x) applies for any control messages e.g., to request bandwidth. The wake-up time for the transmitter to turn on is typically negligible. The corresponding average transmitter-side power at the ONU with sleep mode is obtained by adapting [36, Eqn. (9)] as

$$P_{t,PON,sleep} = 1.1(\rho P_{ta} + (1 - \rho)P_{ts}) \quad (33)$$

where $\rho = \lambda/\mu$. The sleep state power P_{ts} is again taken as a percentage of the active state power P_{ta} (same as in the receiver).

Computation of the power consumption of the LAN transmitter components with sleep mode is slightly different because the transmitter (Tx) side on LAN has an additional duty, namely to send the notifications during the probe state, which does not apply for the PON.

$$P_{t,LAN,sleep} = \frac{1}{\mathbb{E}[C]} \left(\mathbb{E}[B]P_{ta} + (\mathbb{E}[I] - 2 * T_{tw})P_{ts} + 2 * T_{tw} \left(\frac{P_{ts} + P_{ta}}{2} \right) + e^{-\lambda T_t} * T_p * P_{ta} \right) \quad (34)$$

$\mathbb{E}[I]$ is calculated from (4) in [36]; P_{ta} , P_{ts} , and T_{tw} take the same values as their receiver counterparts P_{ra} , P_{rs} , and T_{rw} respectively; the other parameters were already introduced above.

Finally, to compute the total savings in the PON interface (considering both receiver and transmitter), we weight the individual savings above according to the power contributions. For OE optics and OE electronics, this is calculated from the detailed split of sub-components. For digital SoC, we assume 50% weight each for transmitter and receiver. This approach holds because of the following.

$$P_8 = P_{r,8} + P_{t,8} = \alpha P_8 + (1 - \alpha)P_8 \quad (35)$$

where P is the total power, P_r and P_t are power for receiver and transmitter respectively, and α is the weight of the receive power (listed in Table V). If we now apply sleep mode, let us suppose S_r and S_t are the savings factors computed for the

receiver and transmitter respectively. Then, the total power with sleep mode is

$$\begin{aligned} P_{9,hp} &= (\alpha P_{8,hp}) S_{r,hp} + ((1 - \alpha)P_{8,hp}) S_{t,hp} \\ &= (\alpha S_{r,hp} + (1 - \alpha)S_{t,hp}) P_{8,hp} \end{aligned} \quad (36)$$

with

$$hp \in \{HO, HE, HD\} \quad (37)$$

In the LAN, we distinguish between optics and electronics (analog electronics + SerDes) to calculate sleep savings in a similar manner. From (25), where the first term is the optical power, and taking into account the savings from (27), we derive that optics contribute 7 percent to the PtP TRx power, and electronics the remaining 93 percent. Further, we should account for the fact that power shedding was already included in the baseline transceiver power, and the sleep saving factor should only reflect the additional savings from using sleep mode in time periods when power shedding (ps) is not possible. Building on formula (10), we can derive the average consumption when sleep and power shedding are combined from that when only power shedding is used as follows:

$$P_{ps+sleep} = P_{ps} * \frac{P_{sleep}/P_{active} * 10/24 + 0.1 * 14/24}{0.475} \quad (38)$$

P_{sleep}/P_{active} is replaced by the appropriate factor for optics and electronics derived from Table V (derivation analogous to (36)). Substituting these values in (38) and combining with the weights for optics and electronics, this results in

$$\begin{aligned} P_{9,HL} &= P_{8,HL} * (0.19 * 0.07 + 0.37 * 0.93) \\ &= P_{8,HL} * 0.354 \end{aligned} \quad (39)$$

b) OLT sleep modes: Sleep savings are less pronounced in the OLT than in the ONU, resulting in an estimated 20 percent savings in digital processing (note that this is co-located with the ER):

$$P_{9,TD} = P_{8,TD} * 0.80 \quad (40)$$

c) ER sleep modes: Sleep savings in the ER apply to the routing functionalities, excluding the contribution from CBI termination (2.5 percent of the power in the numerator of (23)). By powering off stand-by elements of the router, 34.6 percent power savings can be achieved, resulting in the following overall savings in the ER power component:

$$\begin{aligned} P_{9,ER} &= P_{8,ER} * (0.654 * 0.975 + 1 * 0.025) \\ &= P_{8,ER} * 0.662 \end{aligned} \quad (41)$$

V. RESULTS: POWER REDUCTION AND ENERGY EFFICIENCY IMPROVEMENT

When we apply the saving factors in Table IV sequentially, from the top row to the bottom row, we can now easily calculate the *power per subscriber* for a number of access scenarios. Figure 4 shows the incremental power consumption reduction resulting from all technologies: first introducing only BAU improvements; then additionally introducing cascaded bit-interleaving (CBI), virtual home gateway (vHGW), the

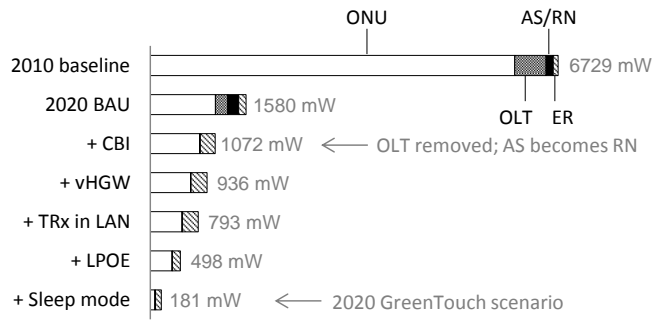


Fig. 4. Green Meter results: power per subscriber after sequential introduction of energy-saving technologies. The power per subscriber is 37 times lower in the GreenTouch scenario compared to the baseline scenario.

redesigned optical transceiver (TRx), LPOE and finally, introducing sleep mode on top of all the other technologies to reach the GT 2020 scenario.

The results show that the average power consumption per subscriber (considering both the access and metro sections) is already reduced by a factor 4.3x, cutting 77 % of the initial power, when considering only BAU improvements and despite strong traffic growth. This is because standard GPON capacity suffices to serve user requirements up to 2020 in the BAU scenario, and hardware advancements following Moore’s law and the use of power shedding strongly reduce ONU power consumption.

Taking energy savings even further by introducing the GreenTouch network architecture and technologies brings together an additional improvement factor 8.7x, resulting in a total power reduction factor 37x, or cutting 97 % of the initial power.

While power per subscriber is a good metric to get an idea of the absolute power consumption of the network, it doesn’t capture the improvement in network performance that is achieved in the 2020 scenarios. This is why we should also consider the *energy efficiency (EE)* improvement. EE in this context is a measure of the traffic that can be transmitted through the access network per unit of energy consumed:

$$EE = \frac{\text{traffic transmitted (kb)}}{\text{energy consumed (J)}} \quad (42)$$

This can be calculated as the total amount of traffic transmitted over a given period (e.g. a year) divided by the total energy consumed in the network in that period, or, equivalently, using the average traffic rates and power consumption values that were given earlier in this work:

$$EE = \frac{\text{average total traffic rate per subscriber (kb/s)}}{\text{power per subscriber (W = J/s)}} \quad (43)$$

We make the calculation for the baseline, BAU and GreenTouch scenario in Table VI. The factor 257x is the product of three contributions: 4.9x improvement due to traffic increase⁷;

⁷If we were to use the 2010 baseline equipment to dimension the network for 2020 traffic load, some components would require more power as shown in line *Power increase due to traffic growth* in Table IV, but EE would improve because the nominator in (42) increases more than the denominator, so the overall factor is an improvement in EE.

TABLE VI
ENERGY EFFICIENCY IMPROVEMENT IN BAU AND GREENTOUCH SCENARIO

	2010 baseline	2020 BAU	2020 GT
Average DS+US traffic rate per subscriber (kb/s)	138	955	955
Power per subscriber (W)	6.73	1.58	0.18
Energy efficiency (kb/J)	21	604	5271
Improvement factor	-	29x	257x

6x business-as-usual improvement; and 8.7x additional improvement from GreenTouch solutions.

VI. CONCLUSION

The Green Meter model for fixed access, developed by the GreenTouch consortium, provides an end-to-end framework for the evaluation of various energy-saving approaches in optical access networks, starting from a baseline scenario in 2010 and providing estimates for future scenarios in 2020.

In this paper, we described the model in detail, showing how the network power consumption is broken down into components (ONU, OLT, AS, and ER) and sub-components (optics, electronics, and digital processing), to which appropriate saving factors are applied. Estimates for all saving factors were given (Table IV) and motivated. We emphasized that the saving factors in Table IV can only be applied sequentially due to complex interactions between the strategies. However, from the detailed description in the text the net effect of individual strategies can be derived.

The main outcome of this model is the evaluation of energy efficiency for two optical access scenarios for 2020: business-as-usual (BAU) and GreenTouch (GT).

In the BAU scenario current trends in energy efficiency are continued until 2020 without specific focus on reducing the energy consumption of access networks. This scenario incorporates Moore’s law, power shedding, efficient hardware design, and efficient cooling. As a result, power per subscriber is reduced 4.3-fold with respect to the 2010 baseline power, and energy efficiency (taking into account traffic growth) improves 29-fold.

The ultimate goal of this analysis was to see what savings are possible if more attention is paid to energy efficiency in the future network design. In the GT scenario, on top of BAU improvements we introduce a cascaded bit-interleaving (CBI) architecture, virtual home gateway (vHGW), redesigned point-to-point (PtP) transceiver (TRx), low-power optics and electronics (LPOE) and sleep modes. As such, the power per subscriber is reduced 37-fold with respect to the 2010 baseline, and energy efficiency improves 257-fold, showing that an emphasis on green network design can indeed have a huge impact on network energy consumption.

ACKNOWLEDGMENT

This research was performed in the context of GreenTouch. Sofie Lambert is funded by the Agency for Innovation by Science and Technology in Flanders (IWT).

REFERENCES

- [1] S. Lambert, W. V. Heddeghem, W. Vereecken, B. Lannoo, D. Colle, and M. Pickavet, "Worldwide electricity consumption of communication networks," *Optics Express*, vol. 20, no. 26, pp. B513–B524, Dec 2012.
- [2] "GreenTouch final results from Green Meter research study: reducing the net energy consumption in communication networks by up to 98 percent by 2020," white paper, August 2015. [Online]. Available: <https://s3-us-west-2.amazonaws.com/belllabs-microsite-greentouch/uploads/documents/White%20Paper%20on%20Green%20Meter%20Final%20Results%20August%202015%20Revision%20-%20vFINAL.pdf>
- [3] P. Vetter, L. Lefevre, L. Gasca, K. Kanonakis, L. Kazovsky, B. Lannoo, A. Lee, C. Monney, X. Z. Qiu, F. Saliou, and A. Wonfor, "Research roadmap for green wireline access," in *2012 IEEE International Conference on Communications (ICC)*, June 2012, pp. 5941–5945.
- [4] P. Vetter, T. Ayhan, K. Kanonakis, B. Lannoo, K. Lee, L. Lefevre, C. Monney, F. Saliou, and X. Yin, "Towards energy efficient wireline networks, an update from greentouch," in *2013 18th OptoElectronics and Communications Conference held jointly with 2013 International Conference on Photonics in Switching*. Optical Society of America, 2013, pp. WP4–2. [Online]. Available: http://www.osapublishing.org/abstract.cfm?URI=OECC_PS-2013-WP4_2
- [5] S. K. Korotky, "Semi-empirical description and projections of Internet traffic trends using a hyperbolic compound annual growth rate," *Bell Labs Technical Journal*, vol. 18, no. 3, pp. 5–21, dec 2013. [Online]. Available: <http://ieeexplore.ieee.org/lpdocs/epic03/wrapper.htm?arnumber=6772725>
- [6] Cisco, "Cisco visual networking index: Forecast and methodology, 2010-2015," white paper, June 2012.
- [7] —, "Cisco visual networking index: Forecast and methodology, 2011-2016," white paper, May 2012.
- [8] Telegeography, "GlobalComms: Broadband statistics - world and regional totals (2004-2011)," <http://www.telegeography.com/products/globalcomms>, accessed July 2012.
- [9] "GreenTouch architecture, technologies and Green Meter assessment for fixed access networks," white paper, March 2016. [Online]. Available: https://s3-us-west-2.amazonaws.com/belllabs-microsite-greentouch/uploads/documents/White_Paper_on_GreenTouch_Fixed_Access.pdf
- [10] D. Suvakovic, H. Chow, D. van Veen, J. Galaro, B. Farah, N. Anthapadmanabhan, P. Vetter, A. Dupas, and R. Boislaigue, "Low energy bit-interleaving downstream protocol for passive optical networks," in *Online Conference on Green Communications (GreenCom), 2012 IEEE*, Sept 2012, pp. 26–31.
- [11] C. Van Praet, H. Chow, D. Suvakovic, D. V. Veen, A. Dupas, R. Boislaigue, R. Farah, M. F. Lau, J. Galaro, G. Qua, N. P. Anthapadmanabhan, G. Torfs, X. Yin, and P. Vetter, "Demonstration of low-power bit-interleaving TDM PON," *Opt. Express*, vol. 20, no. 26, pp. B7–B14, Dec 2012. [Online]. Available: <http://www.opticsexpress.org/abstract.cfm?URI=oe-20-26-B7>
- [12] X. Yin, H. Chow, A. Vyncke, D. Suvakovic, G. Torfs, A. Duque, D. Van Veen, M. Verbeke, T. Ayan, and P. Vetter, "CBI: a scalable energy-efficient protocol for metro/access networks," in *2014 IEEE Online Conference on Green Communications (OnlineGreenComm)*. IEEE, 2014, pp. 126–131.
- [13] J.-P. Gelas, L. Lefevre, T. Assefa, and M. Libsies, "Virtualizing home gateways for large scale energy reduction in wireline networks," in *Electronics Goes Green 2012+ (EGG), 2012*, Sept 2012, pp. 1–7.
- [14] "New GreenTouch innovations to reduce energy consumption in wireline access communications networks by 46 percent," GreenTouch Press Release, November 2014.
- [15] K.-L. Lee, B. Sedighi, R. S. Tucker, H. K. Chow, and P. Vetter, "Energy efficiency of optical transceivers in fiber access networks [invited]," *J. Opt. Commun. Netw.*, vol. 4, no. 9, pp. A59–A68, Sep 2012. [Online]. Available: <http://jocn.osa.org/abstract.cfm?URI=jocn-4-9-A59>
- [16] B. Sedighi, J. Li, K.-L. Lee, S. Gambini, H. Chow, and R. Tucker, "Energy-efficient optical links: Optimal launch power," *Photonics Technology Letters, IEEE*, vol. 25, no. 17, pp. 1715–1718, Sept 2013.
- [17] K.-L. Lee, J. Li, C. A. Chan, N. P. Anthapadmanabhan, and H. K. Chow, "Energy-efficient technologies for point-to-point fiber access," *Optical Fiber Technology*, vol. 26, Part A, pp. 71 – 81, 2015, next Generation Access Networks. [Online]. Available: <http://www.sciencedirect.com/science/article/pii/S1068520015001054>
- [18] J. Li, K.-L. Lee, C. A. Chan, N. P. Anthapadmanabhan, N. Dinh, and P. Vetter, "Dynamic power management at the access node and customer premises in point-to-point and time-division optical access," *Selected Areas in Communications, IEEE Journal on*, vol. 32, no. 8, pp. 1575–1584, Aug 2014.
- [19] Optocom, "InGaAs PINTIA Photodiode Module With LC ROSA (OPX1455-LRO): Data sheet." [Online]. Available: <http://www.optocom.com/OPX1455-LRO.pdf>
- [20] Maxim, "155Mbps Burst-Mode Laser Driver (MAX3643): Data sheet." [Online]. Available: <https://datasheets.maximintegrated.com/en/ds/MAX3643.pdf>
- [21] Broadlight, "Broadlight 2345 SFU ONT: Data sheet."
- [22] Institute for the Energy - Renewable Energy Unit, "Code of Conduct on Energy Consumption of Broadband Equipment Version 4," February 2011.
- [23] Optocom, "InGaAs PINTIA Photodiode Module With FC Receptacle (OPX1355-FRE): Data sheet." [Online]. Available: <http://www.optocom.com/OPX1355-FRE.pdf>
- [24] J. Put, X. Yin, J. Gillis, X. Z. Qiu, J. Bauwelinck, J. Vandewege, H. G. Krimmel, and P. Vetter, "10 Gbit/s burst-mode limiting amplifier with switched time constants for fast settling and large CID tolerance," *Electronics Letters*, vol. 47, no. 17, pp. 970–972, August 2011.
- [25] S. Borkar, "Major challenges to achieve exascale performance," in *Salishan Conf. on High-Speed Computing*, 2009.
- [26] M. E. Lee, W. J. Dally, R. Farjad-Rad, H.-T. Ng, R. Senthinathan, J. Edmondson, and J. Poulton, "CMOS high-speed I/Os-present and future," in *Computer Design, 2003. Proceedings. 21st International Conference on*. IEEE, 2003, pp. 454–461.
- [27] ITU-T, "G-series recommendations supplement 45: GPON power conservation," May 2009. [Online]. Available: <https://www.itu.int/rec/T-REC-G.Sup45-200905-I>
- [28] B. Skubic and D. Hood, "Evaluation of onu power saving modes for gigabit-capable passive optical networks," *IEEE Network*, vol. 25, no. 2, pp. 20–24, March 2011.
- [29] W. Van Heddeghem, B. Lannoo, D. Colle, M. Pickavet, and P. De-meester, "A quantitative survey of the power saving potential in IP-over-WDM backbone networks," *IEEE Communications Surveys and Tutorials*, vol. 18, no. 1, pp. 706–731, 2016.
- [30] A. Vyncke, G. Torfs, C. V. Praet, M. Verbeke, A. Duque, D. Suvakovic, H. Chow, and X. Yin, "The 40 Gbps cascaded bit-interleaving PON [invited]," *Optical Fiber Technology*, vol. 26, pp. 108 – 117, October 2015, next Generation Access Networks. [Online]. Available: <http://www.sciencedirect.com/science/article/pii/S1068520015000929>
- [31] OKI Electronics Components, "OL5157M 1550 nm 40 Gb/s EA Modulator Integrated DFB Laser: Data sheet."
- [32] Hittite, "32 Gbps Limiting Amplifier (HMC865LC3C): Data sheet," March 2011.
- [33] —, "32 Gbps Limiting Amplifier (HMC866LC3C): Data sheet," March 2011.
- [34] Vitesse, "VSC8479 9.95 Gbps to 11.3 Gbps 16-bit Transceiver: Data sheet."
- [35] J. Li, K. L. Lee, and H. K. Chow, "A "power-on-demand" optical transceiver design for green access and in-home network applications," in *Optical Communication (ECOC), 2015 European Conference on*, Sept 2015, pp. 1–3.
- [36] N. P. Anthapadmanabhan, N. Dinh, A. Walid, and A. J. van Wijngaarden, "Analysis of a probing-based cyclic sleep mechanism for passive optical networks," in *Global Communications Conference (GLOBECOM), 2013 IEEE*, Dec 2013, pp. 2543–2548.